Quasi-*a priori* truncation error estimation and higher order extrapolation for non-linear partial differential equations.

F. Fraysse, E. Valero, G. Rubio

E.T.S.I.Aeronáuticos (Universidad Politécnica de Madrid)
Ciudad Universitaria, E-28040 Madrid, Spain

Abstract

In this paper, we show how to accurately estimate the local truncation error of partial differential equations in a quasi-*a priori* way. We approximate the spatial truncation error using the τ-estimation procedure, which aims to compare the discretisation on a sequence of grids with different spacing. While most of the works in the literature focused on an *a posteriori* estimation, the following work develops an estimator for non-converged solutions. First, we focus the analysis on one- and two-dimensional scalar non-linear test cases to examine the accuracy of the approach using a finite difference discretisation. Then, we extend the analysis to a two-dimensional vectorial problem: the Euler equations discretised using a finite volume vertex-based approach. Finally, we propose to analyse a direct application: τ-extrapolation based on non-converged τ-estimation. We demonstrate that a solution with an improved accuracy can be obtained from a non-*a posteriori* error estimation approach.

Keywords: quasi-*a priori* truncation error, finite volume solvers, multigrid, uncertainty estimator

1. Introduction

In the past decades, due to the increasing demand for complex fluid flow simulations, great effort has been done by the Computational Fluid Dynamics (CFD) community in order to increase the accuracy and reduce the calculation costs. It is now well understood that numerical errors play a crucial role in the balance between accuracy and computational time.

The errors commited in solving numerically a set of Partial Differential Equations (PDE) can be broadly classified into three categories:

- Discretisation errors (DE). These errors arise when the mathematical problem is solved numerically on discrete domains. The discretisation error is defined as the difference between the exact solution to the PDE and the exact solution to the discretised PDE.
- Truncation errors (TE). They act as a source for the DE through the *discretisation error transport equation* (DETE, see Roy [1]). The truncation error is defined as the difference between the discrete and continous PDE both applied to the exact solution of the mathematical model.

- Iteration errors (IE). Iterative error is present in a solution when an iterative procedure is used to solve the discrete equations. The iteration error is defined as the difference between the exact solution to the discrete equations and the solution at the current iteration.

The estimation of the numerical error provides valuable information that can be used in different applications. The truncation/discretisation errors are directly related to the mesh distribution, and thus, a careful estimation might be employed in mesh generation/mesh adaptation. These estimations might also be used to increase the accuracy of the partial differential equation solution. However, the accurate evaluation of numerical errors is a challenging task.

The most commonly used strategy to study discretisation errors is based on Richardson extrapolation [2]. Richardson extrapolation is derived from a power series expansion of the numerical solution expanded about the exact solution to the PDE, thus, it assumes a smooth solution in the asymptotic range. The success of Richardson extrapolation [3, 4, 5, 6, 7, 8] is due to its generality as it can be applied to any set of PDE independently of the numerical scheme. Because it is an *a posteriori* error estimator, the method is not code intrusive and relatively easy to implement. However, this approach requires the computation of at least three numerical solutions, on grid of different spacing, in order to obtain the expression of the leading term of the Taylor series. Therefore, this makes this method hardly suitable for complex three-dimensional industrial applications. Another family of discretisation error estimators comes from the solution of auxiliary equations like the DETE (Shih [9]) or the adjoint equations [10, 11]. While these methods proved to be very reliable estimators, they however suffer from a very high computational cost and are code intrusive.

The analysis of truncation error can be done in two manners. First, by deriving analytically the Taylor series expansions [12, 13, 14, 15, 16]. This approach allows for an *a priori* analysis and gives very valuable information on the quality of the mesh and on the accuracy of the numerical scheme. However, the complexity of the related expressions for general three-dimensional non-linear problems together with the dependence on the numerical scheme have prevented the expansion of this approach. The second way of studying the truncation error arised from the multigrid theory [5] and is known as τ-estimation. Given an exact (converged) solution to the discrete PDE, this method relies on the evaluation of the discrete PDE operator on a coarser mesh [4, 17, 18, 19, 20]. Because of its strong relation to mesh quality and accuracy, a careful estimation can yield an increase in the order of the scheme (procedure known as τ-extrapolation) and/or a reliable mesh adaptation indicator [21, 22]. However, truncation error estimation by τ-estimation has always been used *a posteriori*, from converged solutions.

Here, we propose to extend the work of Bernert [18], Fulton [19] and Fraysse *et al.* [20, 23], who focused their study on converged solutions, to non-converged solutions. We develop a truncation error estimator and derive all of the necessary conditions to ensure accuracy. We discuss the conditions for an accurate estimation as follows: the order of the transfer operators acting in the truncation error estimator formula as a function of the order of the numerical scheme, the influence of distortion and the influence of the iteration error on the accuracy of the estimation. In a second step, a τ-extrapolation formula is presented accounting for the above conditions. Whereas non-converged τ-estimation/τ-extrapolation are performed on one- and two-dimensional scalar equations using a finite difference method, a concrete application using the finite volume vertex-based DLR TAU-Code [24] for the Euler equations is subsequently presented.

The present paper is organised as follows. First, we derive in Sec. 2 the mathematical formulation and the conditions to be fulfilled for an accurate τ-estimation/τ-extrapolation for non-converged solutions. In Sec. 3.1 and 3.2, we study the accuracy of the τ-estimation/τ-

extrapolation for non-converged solutions of one-dimensional and two-dimensional reference problems. We present the difficulties associated with this methodology as well as different solutions. Finally, in Sec. 4, we address more realistic configurations with Euler equations on quadrilateral- and triangle-based grids.

2. Problem formulation

Let us consider the discretisation of a partial differential equation on a grid Ω^h indexed by a mesh size parameter h of the following form:

$$\mathcal{A}^h(u^h) = f^h := \mathcal{I}^h f \tag{1}$$

where, $\mathcal{I}^h$ represents a continuum-to-grid Ω^h transfer for the specified f (e.g., pointwise restriction) and u^h represents the converged numerical solution. The discretisation error ϵ^h and the local truncation error τ^h corresponding to Eq. 1 are defined as follows:

$$\begin{aligned} \epsilon^h &= \mathcal{I}^h u - u^h \\ \tau^h &= \mathcal{A}^h(\mathcal{I}^h u) - \mathcal{I}^h \mathcal{A}(u) \end{aligned} \tag{2}$$

In addition to the discrete equation Eq. 1 and considering a full approximation storage multigrid algorithm [5], the coarse grid equation may be written as follows:

$$\mathcal{A}^H(\hat{u}^H) = \mathcal{A}^H(\hat{\mathcal{I}}_h^H \tilde{u}^h) + \mathcal{I}_h^H(f^h - \mathcal{A}^h(\tilde{u}^h)), \qquad \hat{u}^H \approx \hat{\mathcal{I}}_h^H(\epsilon_{it}^h + \tilde{u}^h) \tag{3}$$

corresponding to the discrete equation on a coarser mesh Ω^H, with a mesh ratio of $\rho = h/H < 1$. In Eq. 3, $\tilde{u}^h$ is the current approximation of the solution (relaxed on the fine grid and not necessarily converged), $\epsilon_{it}^h = u^h - \tilde{u}^h$ is the fine grid iteration error, for which its high frequencies must be smoothed, $\hat{I}_h^H$ represents the fine to coarse transfer operator of the solution, whereas I_h^H represents the fine to coarse transfer operator of the residual. Note that these restriction operators are not necessarily identical. Similarly, introducing the *relative truncation error* τ_h^H, Eq. 3 may be written as follows:

$$\mathcal{A}^H(\hat{u}^H) = f^H + \tau_h^H \quad \text{with} \tag{4}$$

$$\tau_h^H = (\mathcal{A}^H(\hat{\mathcal{I}}_h^H \tilde{u}^h) - f^H) - \mathcal{I}_h^H(\mathcal{A}^h(\tilde{u}^h) - f^h) = T1 + T2 \tag{5}$$

Our goal is to use τ_h^H to estimate τ^H. If this estimation can be performed with sufficient accuracy, then one can use this local error as a mesh adaptation indicator, as an uncertainty estimator or as a means to increase the order of accuracy of the spatial scheme.

The following theorem provides the relationship between the accuracy of τ_h^H towards τ^H and the order of the restriction operators acting in Eq. 5.

Theorem 1 (Truncation Error Estimate)**.** *Assume that there exists $n, p, q, s \geq 1$ such that if u is of class $C^{n+p+q}(\Omega)$, the truncation error (2) satisfies:*

- ***(A1)*** *Local truncation error of order p: $\tau^h = h^p \mathcal{I}^h v + O(h^{p+q})$, with v of class $C^q(\Omega)$*
- ***(A2)*** *Local discretisation error of order p: $\epsilon^h = h^p \mathcal{I}^h w + O(h^{p+q})$, with w of class $C^q(\Omega)$*
- ***(A3)*** *Fine to coarse transfer operator of the solution of order s: $\hat{\mathcal{I}}_h^H \mathcal{I}^h \phi = \mathcal{I}^H \phi + O(h^s)$, with ϕ of class $C^s(\Omega)$*

then

$$\tau_h^H = (1-\rho^p)\tau^H + \mathcal{I}_h^H \left.\frac{\partial \mathcal{A}^h}{\partial u^h}\right|_{\tilde{u}^h} \epsilon_{it}^h - \left.\frac{\partial \mathcal{A}^H}{\partial u^H}\right|_{\hat{\mathcal{I}}_h^H \tilde{u}^h} \hat{\mathcal{I}}_h^H \epsilon_{it}^h + O(\max(h^{\min(s,p+q)}, \|\epsilon_{it}^h\|^2)) \tag{6}$$

where $\frac{\partial \mathcal{A}^h}{\partial u^h}$ and $\frac{\partial \mathcal{A}^H}{\partial u^H}$ represent the Jacobian on the fine and coarse grids.

Proof of this theorem can be found in Fraysse *et al.* [20].

Corollary 1 (Dynamic τ-extrapolation)**.** *Let us consider the problem*

$$\mathcal{A}^H(\overline{u}^H) = f^H + \frac{1}{1-\rho^p}\tau_h^H \tag{7}$$

and assume that,

- ***(A4)*** *Fine to coarse transfer operator of the residual such that:*

$$\mathcal{I}_h^H = \left.\frac{\partial \mathcal{A}^H}{\partial u^H}\right|_{\hat{\mathcal{I}}_h^H \tilde{u}^h} \hat{\mathcal{I}}_h^H \left(\left.\frac{\partial \mathcal{A}^h}{\partial u^h}\right|_{\tilde{u}^h} \right)^{-1}$$

Then it follows,

$$\overline{\epsilon}^H = \mathcal{I}^H u - \overline{u}^H = O(\max(h^{\min(s,p+q)}, \|\epsilon_{it}^h\|^2, h^p \|\epsilon_{it}^h\|)) \tag{8}$$

Proof. Let us first derive the DETE,

$$\begin{aligned}
\tau^H \quad = \quad & \mathcal{A}^H(\mathcal{I}^H u) - \mathcal{I}^H \mathcal{A}(u) = \\
& \mathcal{A}^H(\mathcal{I}^H u) - \mathcal{A}^H(u^H) = \\
& \mathcal{A}^H(\mathcal{I}^H u) - \mathcal{A}^H(\mathcal{I}^H u - \epsilon^H) = \\
& \left.\frac{\partial \mathcal{A}^H}{\partial u^H}\right|_{\mathcal{I}^H u} \epsilon^H + O(\|\epsilon^H\|^2) = \\
& \left.\frac{\partial \mathcal{A}^H}{\partial u^H}\right|_{\hat{\mathcal{I}}_h^H(\tilde{u}^h + \epsilon^h + \epsilon_{it}^h + O(h^s))} \epsilon^H + O(h^{2p}) = \\
& \left.\frac{\partial \mathcal{A}^H}{\partial u^H}\right|_{\hat{\mathcal{I}}_h^H \tilde{u}^h} \epsilon^H + O(\max(h^{\min(sp,2p)}, h^p \|\epsilon_{it}^h\|))
\end{aligned} \tag{9}$$

The above formulation of the DETE follows the advanced linearisation of Phillips and Roy [26].

From **(A1)**, **(A2)** and Eq. 9 it follows:

$$\tau^H \sim O(H^p), \quad \epsilon^H \sim O(H^p), \quad \tau^H \sim \left.\frac{\partial \mathcal{A}^H}{\partial u^H}\right|_{\hat{I}_h^H \tilde{u}^h} \epsilon^H$$

$$\Rightarrow \quad \left\| \left.\frac{\partial \mathcal{A}^H}{\partial u^H}\right|_{\hat{I}_h^H \tilde{u}^h} \right\|^{-1} \leq M, \qquad \text{with } M \text{ independent of } H \tag{10}$$

Using Eq. 6 and **(A4)**, Eq. 7 can be rewritten as,

$$\mathcal{A}^H(\overline{u}^H) = f^H + \frac{1}{1-\rho^p}\tau_h^H = f^H + \tau^H + O(\max(h^{\min(s,p+q)}, \|\epsilon_{it}^h\|^2)) \tag{11}$$

Then, using DETE Eq. 9, the truncation error $\overline{\tau}^H$ associated to Eq. 7 can be written as,

$$\overline{\tau}^H = O(\max(h^{\min(s,p+q)}, \|\epsilon_{it}^h\|^2)) = \left.\frac{\partial \mathcal{A}^H}{\partial u^H}\right|_{\hat{I}_h^H \tilde{u}^h} \overline{\epsilon}^H + O(\max(h^{\min(sp,2p)}, h^p \|\epsilon_{it}^h\|)) \tag{12}$$

With Eq. 10, Eq. 12 becomes

$$\overline{\epsilon}^H = O(\max(h^{\min(s,p+q)}, \|\epsilon_{it}^h\|^2, h^p \|\epsilon_{it}^h\|)) \tag{13}$$

□

Discussion:

The two first assumptions state that the meshes employed are sufficiently refined so that both discretisation and truncation errors decrease at the formal rate of convergence. Thus, this analysis is only valid in the asymptotic range. The main conclusions of Eq. 6 are related to the order of the restriction operator acting on the solution and on the magnitude of the iteration error. Examining the exponent of the last term in Eq. 6, it can be deduced that it is necessary to use higher order interpolation $s > p$ to transfer the solution from a fine to a coarse mesh. If $s \leq p$, then the truncation error estimation will be dominated by the term $O(h^s)$, reducing the accuracy of the general results of the formula.

Another interesting conclusion of Eq. 6 concerns its dependence on the iteration error. It can be remarked that if **(A4)** holds, then the accuracy of the truncation error estimation increases quadratically when the iteration error decreases until it falls below $O(h^{\min(s,p+q)})$; then an accurate truncation error estimation can be obtained in the early stages of the iteration towards convergence. Once an accurate truncation error estimation is available, Corollary 1 demonstrates that a better approximation of the solution on the coarse grid can be computed.

In the linear case, by denoting $\mathcal{A}^h(u^h) = \mathcal{L}^h u^h$, **(A4)** can be rewritten as:

$$\mathcal{I}_h^H = \mathcal{L}^H \hat{I}_h^H \left(\mathcal{L}^h\right)^{-1} \tag{14}$$

If Eq. 14 is satisfied, it can be remarked that Eq. 6 and Eq. 8 do not depend at all on the iteration error. Actually, the dependence on the iteration error of the higher order terms ($\|\epsilon_{it}^h\|^2$) is due

to the linearisation of the discrete operator $\mathcal{A}^h$, which does not take place if $\mathcal{A}$ is linear. It means that, constructing the restriction operator for the fine grid residual $\mathcal{I}_h^H$ following Eq. 14 yields an accurate truncation error estimation at the first stage of the iteration procedure. However, it is of little practical interest since the fine grid differential operator $\mathcal{L}^h$ has to be inverted, which is equivalent to solving the initial problem.

Another approach to fulfill Eq. 14 would be to compute $\hat{\mathcal{I}}_h^H$ such that,

$$\hat{\mathcal{I}}_h^H = \left(\mathcal{L}^H\right)^{-1} \mathcal{I}_h^H \mathcal{L}^h \tag{15}$$

Eq. 15 only requires the inversion of the coarse grid differential operator $\mathcal{L}^H$, which is much cheaper than solving Eq. 14. However, we remind the reader that the above analysis assumes (**A3**) and there is no guarantee that Eq. 15 yields to an operator $\hat{\mathcal{I}}_h^H$ of order $s > p$, except for special cases that we will not discuss here.

Finally, Eq. 15 could be solved for the coarse grid operator $\mathcal{L}^H$ instead,

$$\mathcal{L}^H = \mathcal{I}_h^H \mathcal{L}^h \left(\hat{\mathcal{I}}_h^H\right)^+ \tag{16}$$

where $\left(\hat{\mathcal{I}}_h^H\right)^+$ stands for the Moore-Penrose pseudo-inverse of $\hat{\mathcal{I}}_h^H$. However in our anaysis, we assumed a *discretisation coarse grid approximation* (dca) [27]. In the dca approach, the coarse grid operator has the same stencil as the fine grid operator, thus the associated truncation errors have the same expressions and (**A1**) and (**A2**) hold both on Ω^h and Ω^H.

On the other hand, for non-linear problems, **(A4)** requires the inversion of the Jacobian which is a common practice when steady state solutions are obtained with an implicit scheme.

To validate Eq. 6 and Eq. 8, we employed a set of partial differential equations with known analytic solutions in the following sections. For each test case, first, an analysis is made on the application of **(A4)** to verify Eq. 6 and second, τ-extrapolation is applied in order to verify Eq. 8. First, we emphasised the analysis on one-dimensional equations, and then we investigated the extension to two-dimensional scalar problems, both solved using a finite difference approach. Finally the two-dimensional Euler equations are considered using a vertex-based finite volume approach.

3. Detailed analysis on reference problems

In this section, we studied the effects on the dynamic truncation error estimation (TEI) of the restriction operator acting on the fine grid residual $\mathcal{I}_h^H$ for different mesh distributions. Emphasis is given on how to get a truncation error estimate from a non-converged solution, while accuracy towards exact truncation error is presented briefly in Appendix A and in more details in Fraysse *et al.* [20]. The truncation error estimate is computed for different iteration error magnitudes and compared against its converged value (TEC) ($\tau_h^H(\tilde{u}^h) - \tau_h^H(u^h)$)). Then, in a second step, τ-extrapolation is applied from instantaneous (DEI) and converged (DEC) truncation error estimates by solving Eq. 7 using distinct restriction operators $\mathcal{I}_h^H$ and the effects on the discretisation error are shown using analytic solutions. In this work, we considered three different operators to restrict from fine to coarse grid, the term T_2 in Eq. 5:

- T_2 is neglected, the approach is referred to as (1)
- T_2 is restricted using injection, the approach is referred to as (2)

- T_2 is restricted following **(A4)**, the approach is referred to as (3)

In order to verify the discretisation error of the initial problems as well as the τ-extrapolation procedure, the Method of Manufactured Solutions [28, 30] (MMS) is used. This method is used extensively in the context of CFD code verification. It consists in defining an analytic solution, and modifying the governing equations accordingly, by adding a source term. This source term is added such that the chosen analytic solution satisfies the governing equations.

Although the form of the manufactured solution is somewhat arbitrary, it should be chosen to be smooth, infinitely differentiable (to avoid the cancelation of higher order derivatives) and realisable (i.e., solutions should be avoided that have negative densities, pressures, and temperatures for example in the case of the Euler equations). Trigonometric functions were employed because no derivative can be eliminated, which is of importance to analyse the order of accuracy.

3.1. One-dimensional non-linear test case

First, to illustrate the ability of the formulation of Eq. 5 to deal with non-converged solutions, we considered the one-dimensional forced Burger's equation with known exact solution.

The one-dimensional equation considered reads as follows:

$$-u'' + uu' = f + b.c \tag{17}$$

where $b.c$ represents the boundary conditions. Furthermore, we considered the following forcing function f and boundary conditions:

$$\begin{cases} f(x) = 16\cos(4x) - 4\sin(4x)\cos(4x) \\ u(0) = u_{ex}(0), \quad u(1) = u_{ex}(1) \end{cases} \tag{18}$$

This problem has the following exact solution:

$$u_{ex}(x) = \cos(4x).$$

Eq. 17 is solved using a second-order spatial scheme. A finite difference method associated with a second-order accurate central scheme for the computation of the first and second derivatives was considered so that (**A1**) and (**A2**) hold with $p = q = 2$ for the uniform and $p = q = 1$ for the distorted grids (see Appendix A). The fine grid was extracted from the coarse grid by inserting a new node in each coarse grid cell. In this way, in order to restrict the solution from fine to coarse grid, an injection operator could be used so that (**A3**) holds with $s = \infty$. Finally, at convergence, it follows that $\frac{1}{1-\rho^p}\tau_h^H - \tau^H \sim O(h^4)$ for the uniform and $\frac{1}{1-\rho^p}\tau_h^H - \tau^H \sim O(h^3)$ for the distorted grids (see Appendix A and Fraysse *et al.* [20]). In order to study the influence of the iteration error, the steady-state solution was reached using a Runge-Kutta relaxation scheme and a multigrid strategy.

We focused the analysis on the influence of the restriction operator acting on the fine grid residual $\mathcal{I}_h^H$, for two different mesh distributions: uniform and distorted grids.

The uniform distribution was generated such that:

$$x_i = \frac{i-1}{\text{imax}-1} \qquad i = 1, ..., \text{imax} \tag{19}$$

while the distorted distribution was constructed in this way:

$$x_i = (i-1)h_{unif} + (\text{rand}(i) - 0.5)h_{unif}^q, \quad h_{unif} = \frac{1}{\text{imax} - 1}, \quad q \geq 1 \tag{20}$$

Here, imax is the maximum number of nodes of the coarse grid Ω^H and the function rand returns a random value between 0 and 1. q controls the skewness of the mesh in the case of distorted grids. In this study, q was set to 1. A representation of the two mesh topologies can be seen in Fig. 1.

τ-estimation using Eq. 5 uses two grid levels of similar characteristics. In order to fulfill this condition the fine grids Ω^h were generated by bisecting all segments of the grids Ω^H. In this way, the requirements for a *systematic mesh refinement* (Oberkampf and Roy [29]), who state that the successively refined grids should satisfy a *uniform refinement* and a *consistent refinement*, were fulfilled.

In order to validate Eq. 6, Eq. 17 was solved on an imax=65 nodes grid for each of the two mesh topologies. At each multigrid cycle, the truncation error estimation from Eq. 5 was computed using either injection for $\mathcal{I}_h^H$ or (**A4**) and compared to its converged value. Results are reported in Fig. 2(a) and Fig. 3(a) for the uniform and distorted grids respectively.

In these graphs, the solver tolerance, the L_2 norms of the converged truncation error estimate (TEC), the iteration error, the squared iteration error, and the difference between the instantaneous truncation error estimate and its converged value (TEI-TEC=$\tau_h^H(\tilde{u}^h) - \tau_h^H(u^h)$)) are represented. TEI-TEC (1) stands for the method one, where the second term of Eq. 5 is neglected. TEI-TEC (2) is the second approach where the term T_2 in Eq. 5 was computed using an injective operator $\mathcal{I}_h^H$. Finally, TEI-TEC (3) means that $\mathcal{I}_h^H$ was computed such that (**A4**) was satisfied. It can be seen for all mesh topologies that neglecting the fine grid residual (second term of Eq. 5) or restricting it using injection does not yield to a quadratic convergence. Typically, $\|\tau_h^H(\tilde{u}^h) - \tau_h^H(u^h))\|_{L_2}$ decreases at the same rate as $\|\epsilon_{it}^h\|_{L_2}$, therefore these former approaches do not allow to reach a faster convergence and the condition that the iteration error (or a typical solver tolerance) be smaller than the truncation error is recovered. However, when $\mathcal{I}_h^H$ fulfills (**A4**) it can be seen that the quantity $\|\tau_h^H(\tilde{u}^h) - \tau_h^H(u^h))\|_{L_2}$ decreases quadratically with the iteration error, which is the result expected from Eq. 6.

Once a truncation error estimate was available through the use of Eq. 5, we performed the so-called τ-extrapolation technique by solving Eq. 7 on grid Ω^H. This procedure has been repeated at each multigrid cycle in order to measure the influence of the iteration error arising from the discretisation of the initial problem on grid Ω^h. As for the verification of Eq. 6, Eq. 8 was checked with and without assumption (**A4**) using the two grid topologies of Eq. 19-20. The results of this analysis are reported in Fig. 2(b) and Fig. 3(b) for the uniform and distorted grids respectively. In these plots, the discretisation errors obtained from the converged solutions on grids Ω^h and Ω^H are also displayed and compared against the τ-extrapolation obtained on Ω^H from a converged (DEC) and non-converged solutions (DEI). The first comment, common to the two mesh topologies, concerns the discretisation error obtained by solving Eq. 7 from a converged τ-estimation. It can be seen that the τ-extrapolation procedure improves substancially the accuracy of the discretised solution. The extrapolated discretisation errors are at least two orders of magnitude smaller than the discretisation error obtained from the initial problem solved on Ω^h. This can be easily explained by remarking that the second term of the Taylor expansions associated to the central discretisations are of order $p+q=4$. Thus, from Eq. 7, the discretisation error associated to Eq. 8 computed from a converged τ-estimation is of order $p+q=4$. The second important comment is related to the discretisation error associated to the extrapolated problem obtained with a dynamic τ-estimation approach. It can be seen that, as a natural consequence of

the dynamic τ-estimation analysis, the same conclusions hold. When (**A4**) does not hold or if the second term of Eq. 5 is neglected, then the discretisation error associated to the extrapolated problem Eq. 8 reaches its converged value at a rate of convergence proportional to $||\epsilon_{it}^h||_{L_2}$, so that no special gain is obtained. However, if (**A4**) holds, it can be seen that the discretisation error associated to Eq. 8 reaches its converged value at a rate proportional to $||\epsilon_{it}^h||_{L_2}^2$, therefore validating Eq. 7.

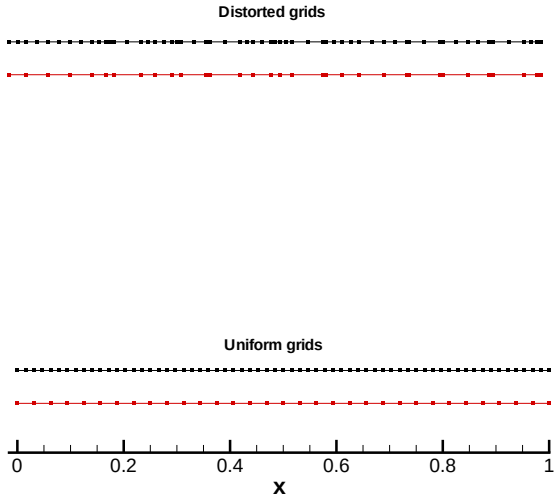

Figure 1: 1D Burgers' equation, uniform and distorted grids.

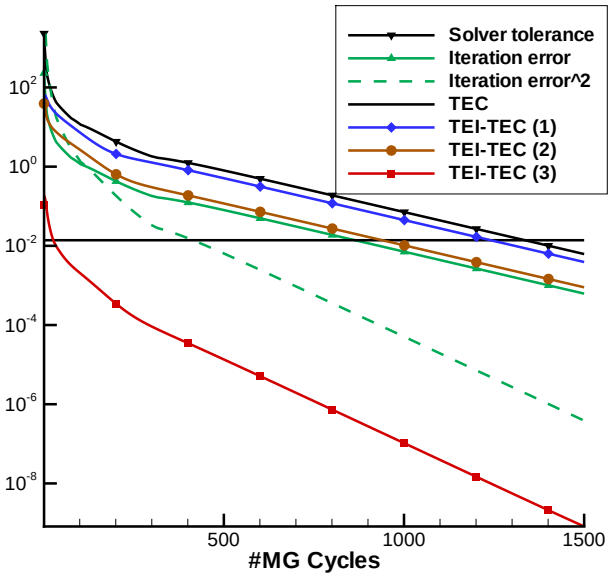

(a)

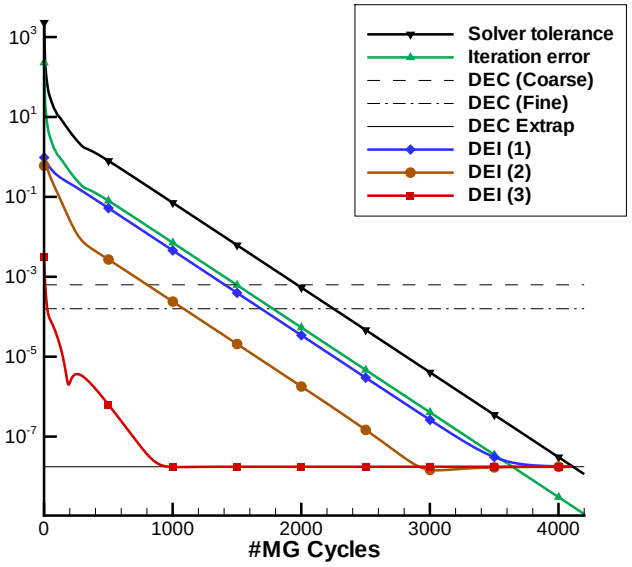

(b)

Figure 2: 1D Burgers' equation, uniform grid. (a): Analysis of dynamic truncation error accuracy and (b) dynamic τ-extrapolation.

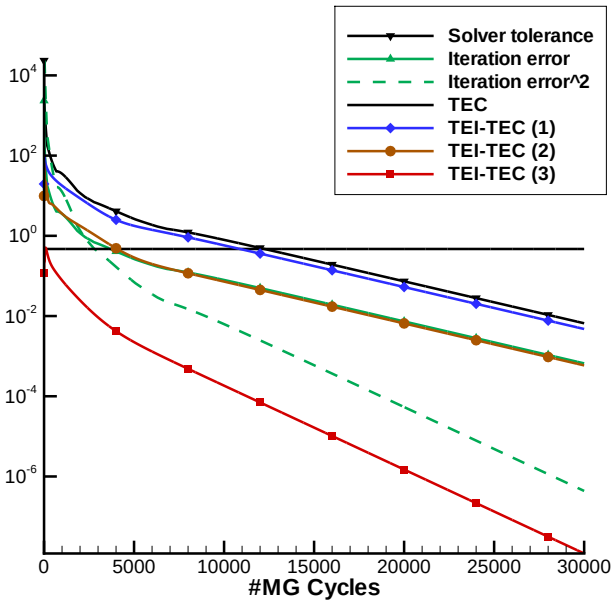

(a)

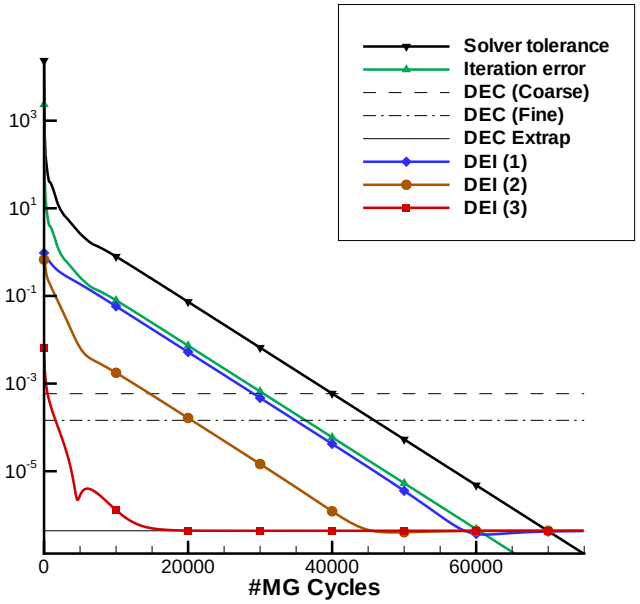

(b)

Figure 3: 1D Burgers' equation, distorted grid. (a): Analysis of dynamic truncation error accuracy and (b) dynamic τ-extrapolation.

3.2. Two-dimensional non-linear test case

The analysis performed for one-dimensional equations was extended in this section to two-dimensional problems. The analysis of Sec. 2 does not make any assumptions on the dimensionality of the problem. However, it states that the discretisation and truncation error have the same formulation both on coarse and fine mesh, requiring some consistency in the topology of both grids. Therefore, under the assumption of topologically similar grids, we indicate in this section that the extension to two-dimensional partial differential equations is straightforward.

As in the previous case, the two-dimensional forced Burger's equation is studied,

$$-\Delta u + u u_x = f + b.c \tag{21}$$

where $b.c$ represents boundary conditions. We considered the following test function and boundary conditions:

$$\begin{cases} f(x,y) = 52\cos(4x+6y) - 4\sin(4x+6y)\cos(4x+6y) \\ u(x,y) = u_{ex}(x,y), \forall (x,y) \in \Omega = [0,1]^2 \end{cases} \tag{22}$$

This problem has the following exact solution:

$$u_{ex}(x,y) = \cos(4x+6y).$$

Similarly to the one-dimensional case, Eq. 21 is solved using a second-order spatial scheme. A finite difference method associated with a second-order accurate central scheme for the computation of the first and second derivatives was considered so that (**A1**) and (**A2**) hold with $p = q = 2$ for the uniform grids and $p = q = 1$ for the distorted grids (see Appendix A). In order to restrict the solution from fine to coarse grid, an injection operator has been used so that (**A3**) holds with $s = \infty$. Finally, at convergence, it follows that $\frac{1}{1-\rho^p}\tau_h^H - \tau^H \sim O(h^4)$ for the uniform and $\frac{1}{1-\rho^p}\tau_h^H - \tau^H \sim O(h^2)$ for the distorted grids (see Appendix A and Fraysse *et al.* [20]). In order to study the influence of the iteration error, the steady-state solution was reached using a Runge-Kutta relaxation scheme and a multigrid strategy.

We focused the analysis on the influence of the restriction operator acting on the fine grid residual $\mathcal{I}_h^H$, for different mesh distributions: uniform and distorted grids. These grid distributions follow Eq. 19-20 and are represented in Fig. 4 (coarse and embedded fine grids). Note that in order to keep an accurate finite difference formulation, the distorted grid case only used a perturbation in the y-direction.

Similarly to the precedent case, our aim was to validate Eq. 6 and Eq. 8. In order to do so, we solved Eq. 21-22 on 65×65 grids using the two aforementioned topologies. At each multigrid cycle, the truncation error estimation Eq. 5 has been computed and added as a source term in the extrapolated problem Eq. 8. The results and conclusions obtained for the one-dimensional problem hold for the two-dimensional test case (see Fig. 5-6). If the second term of Eq. 5 is neglected or restricted with an operator which does not satisfy (**A4**), then the quantity $\|\tau_h^H(\tilde{u}^h) - \tau_h^H(u^h))\|_{L_2}$ decreases at a rate proportional to $\|\epsilon_{it}^h\|_{L_2}$, thus does not yield a substantial gain. However, if $\mathcal{I}_h^H$ is constructed such that (**A4**) holds, then $\|\tau_h^H(\tilde{u}^h) - \tau_h^H(u^h))\|_{L_2}$ decreases quadratically with the iteration error, validating Eq. 6. As a consequence, the τ-extrapolation from dynamic τ-estimation follows the same tendency.

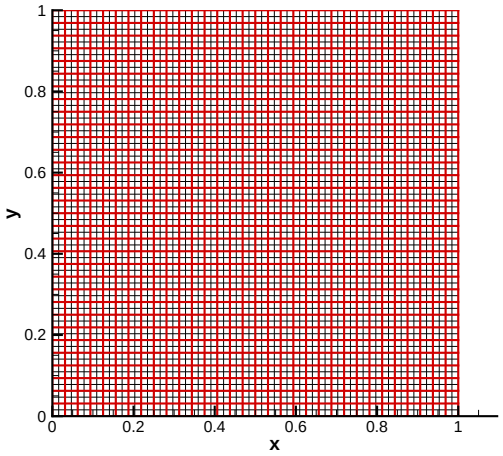

(a)

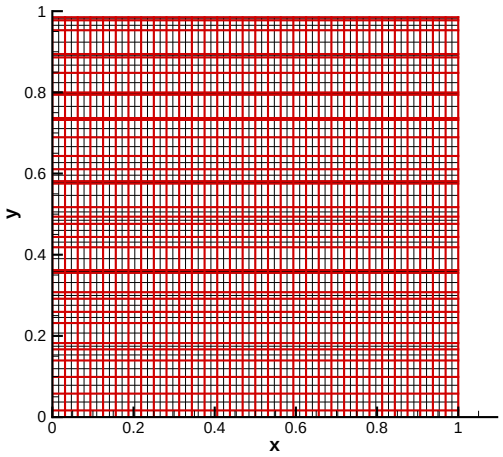

(b)

Figure 4: 2D Burgers' equation, (a): uniform and (b): distorted grids.

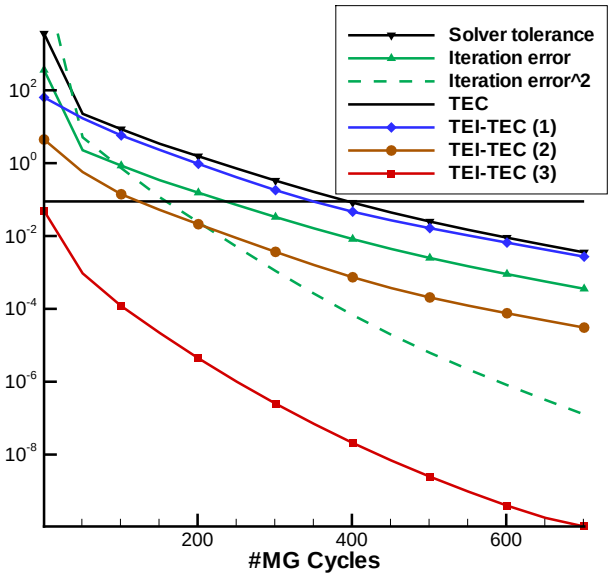

(a)

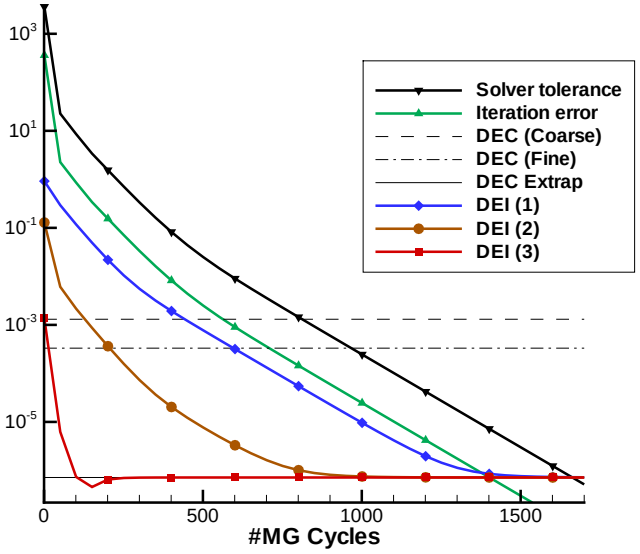

(b)

Figure 5: 2D Burgers' equation, uniform grid. (a): Analysis of dynamic truncation error accuracy and (b) dynamic τ-extrapolation.

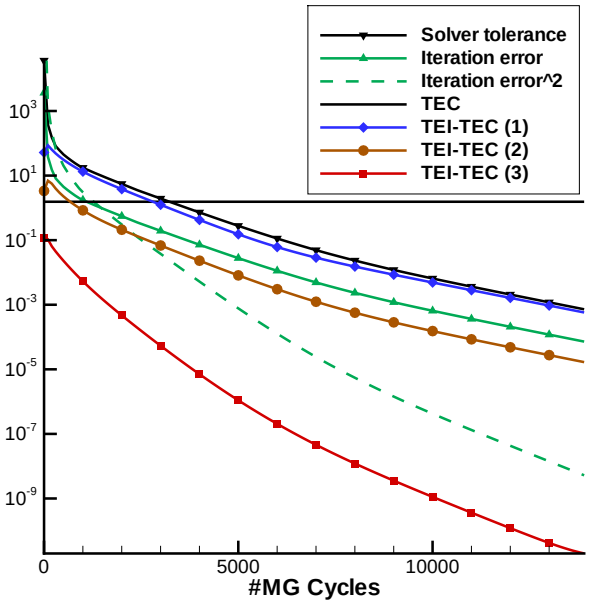

(a)

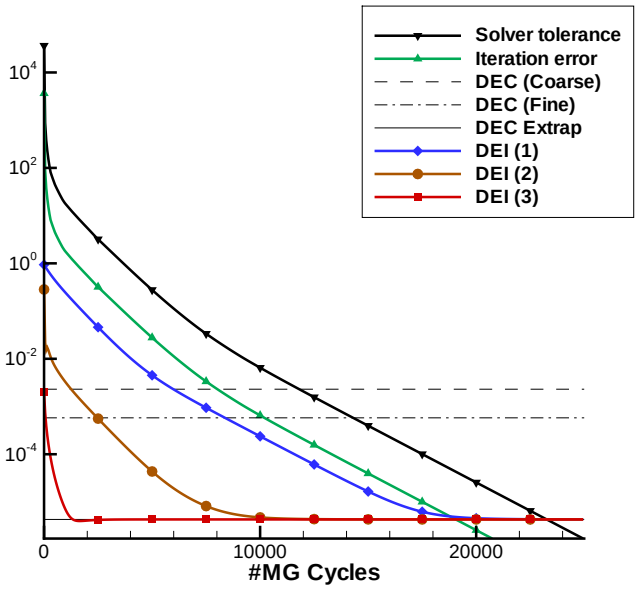

(b)

Figure 6: 2D Burgers' equation, distorted grid. (a): Analysis of dynamic truncation error accuracy and (b) dynamic τ-extrapolation.

4. Numerical experiments on two-dimensional Euler equations

We finished our study by performing an analysis of the dynamic truncation error estimation and extrapolation on the two-dimensional Euler equations, as follows:

$$\frac{\partial \mathbf{U}}{\partial t} + \frac{\partial \mathbf{F}}{\partial x} + \frac{\partial \mathbf{G}}{\partial y} = \mathbf{S} \tag{23}$$

with

$$\mathbf{U} = \begin{pmatrix} \rho \\ \rho u \\ \rho v \\ \rho E \end{pmatrix} \qquad \mathbf{F} = \begin{pmatrix} \rho u \\ \rho u^2 + p \\ \rho uv \\ \rho uH \end{pmatrix} \qquad \mathbf{G} = \begin{pmatrix} \rho v \\ \rho uv \\ \rho v^2 + p \\ \rho vH \end{pmatrix}$$

and

$$p = (\gamma - 1)\left(\rho E - \frac{\rho(u^2 + v^2)}{2}\right) \tag{24}$$

A source term $\boldsymbol{S}$ is added such that the following chosen analytic solution satisfies the governing equations:

$$\begin{aligned} \rho(x, y) &= 1 + \cos(2xy) \\ u(x, y) &= (2 + \cos(4x) - \sin(6y))/10 \\ v(x, y) &= (2 + \cos(4x) + \sin(6y))/12 \\ p(x, y) &= 1 + \cos(2x) + \sin(y) \end{aligned} \tag{25}$$

We solved Eq. 23 and Eq. 24 on quad- and triangle-based geometries using the node-based finite volume DLR TAU-Code [24]. DLR TAU-Code solves the Reynolds Averaged Navier-Stokes equations on unstructured hybrid grids by employing a second-order finite volume discretisation. The multigrid strategy implemented in TAU uses the full approximation scheme algorithm to compute the correction term on the coarse grids. The coarse grids are obtained by agglomeration of the fine grid dual cells (control volumes obtained by joining the barycenters of all connected elements). When the primary grid is composed of quadrilaterals (or hexahedrons for 3D computations), then the advanced front method is capable of agglomerating 4 quadrilaterals (8 hexahedrons) to create a coarse quadrilateral (hexahedron), as in a structured solver. However, when the primary grid is unstructured, the agglomeration algorithm creates coarse grid elements that do not necessarily maintain the fine grid characteristics. In the context of multigrid, this situation is not a strong limitation, particularly in TAU, where the coarse grid fluxes are computed with a first-order accuracy. However, in the context of truncation error estimation, as we discussed earlier, it is of importance that the truncation error is identical between fine and coarse grids (see Fraysse *et al.* [20]). This goal clearly cannot be accomplished if the elements differ from fine to coarse mesh. To circumvent this issue and to obtain estimations of the truncation error for unstructured grids, in the following analysis, the fine mesh (where the flow solution is actually computed) was obtained from the coarse mesh by bisecting all of the edges. In this way, all coarse grid vertices also belong to the fine grid so that this method allows the use of injection to restrict the solution from fine to coarse grids.

Eq. 23 and Eq. 24 have been discretised using the Jameson-Schmidt-Turkel second order scheme [25], so that we expect Eq. 6 to hold with $p = 2, q = 1, s = \infty$. The geometries employed in this study follow the distributions of Eq. 19-Eq. 20 with 65 nodes in each direction (see Fig. 7). Similarly to the previous one- and two-dimensional test cases, we studied the dynamic τ-estimation and τ-extrapolation as a function of the magnitude of the iteration error. Truncation error maps, exact and estimates can be seen in Appendix A. Let us detail the procedure in the case that (**A4**) holds.

For convenience, we rewrite Eq. 5

$$\begin{aligned} \tau_h^H &= (\mathcal{A}^H(\hat{I}_h^H \tilde{u}^h) - f^H) - \left.\frac{\partial \mathcal{A}^H}{\partial u^H}\right|_{\hat{I}_h^H \tilde{u}^h} \hat{I}_h^H \left(\left.\frac{\partial \mathcal{A}^h}{\partial u^h}\right|_{\tilde{u}^h} \right)^{-1} (\mathcal{A}^h(\tilde{u}^h) - f^h) \\ &= T_1 + T_2 \end{aligned} \tag{26}$$

While T_1 can be easily computed, in order to avoid explicit inversion of the Jacobian matrix, T_2 is computed in this way:

- Solve the linear system: $\left.\frac{\partial \mathcal{A}^h}{\partial u^h}\right|_{\tilde{u}^h} \phi_1^h = \mathcal{A}^h(\tilde{u}^h) - f^h$
- Restrict $\tilde{u}$ and ϕ_1^h using $\hat{I}_h^H$
- Multiply by coarse grid Jacobian $T_2 = \left.\frac{\partial \mathcal{A}^H}{\partial u^H}\right|_{\hat{I}_h^H \tilde{u}^h} \hat{I}_h^H \phi_1^h$

In the current analysis, the linear system is solved using the GMRES/ILU routines from the PETSc package [31] using an exact representation of the Jacobian matrix associated to the Jameson-Schmidt-Turkel scheme, already implemented into the DLR TAU-Code. Due to the computational cost, the simulations have been performed for selected solver tolerances $(0.5, 0.1, 0.05, 0.01, 0.005, 0.001)$, instead of at each multigrid cycle for the previous cases. However, as we shall see in the following, this is sufficient in order to verify Eq. 6 and Eq. 7.

Similar conclusion of previous tests are obtained (see Fig. 8-11): if the second term of Eq. 5 is neglected or restricted with an operator which does not satisfy (**A4**), then the quantity $\|\tau_h^H(\tilde{u}^h) - \tau_h^H(u^h))\|_{L_2}$ decreases at a rate proportional to $\|\epsilon_{it}^h\|_{L_2}$, thus does not yield a substantial gain. However, if $\hat{I}_h^H$ is constructed such that (**A4**) holds, then $\|\tau_h^H(\tilde{u}^h) - \tau_h^H(u^h))\|_{L_2}$ decreases quadratically with the iteration error, validating Eq. 6. As a consequence, the τ-extrapolation from dynamic τ-estimation follows the same tendency.

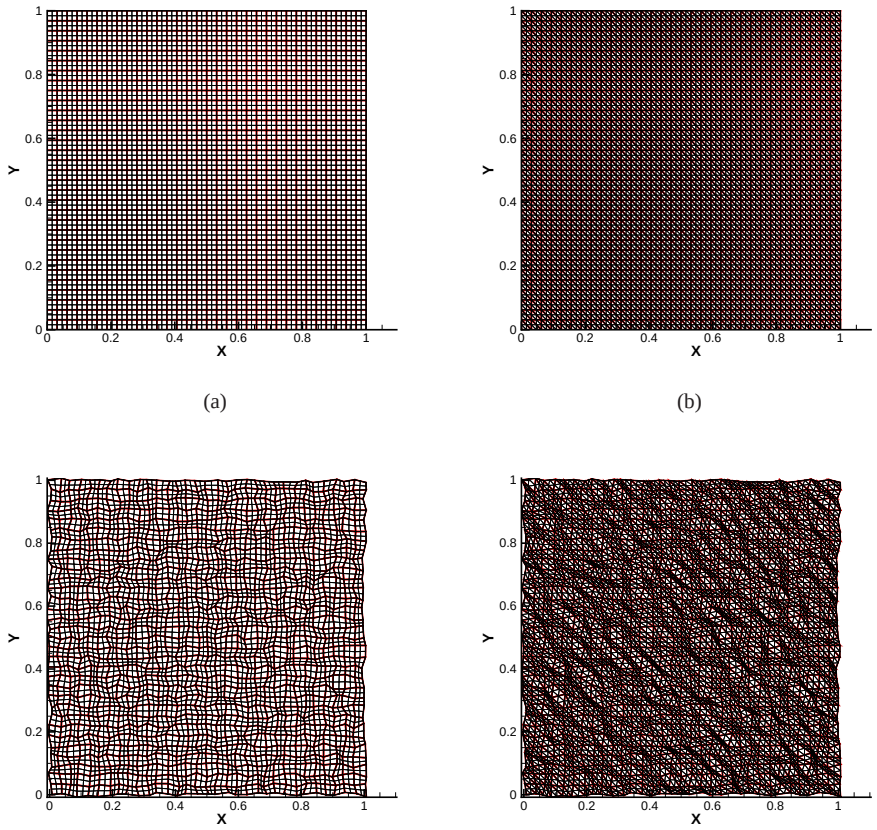

Figure 7: Euler equations, (a): quad-based uniform, (b): triangle-based uniform, (c): quad-based distorted and (d): triangle-based distorted grids.

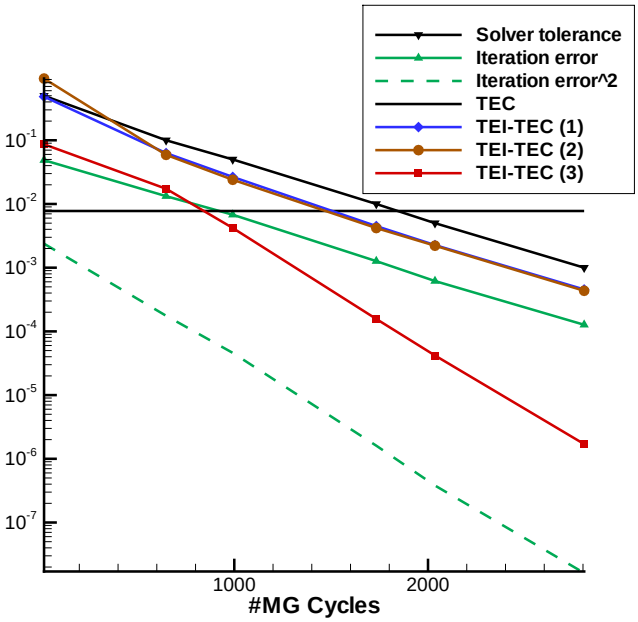

(a)

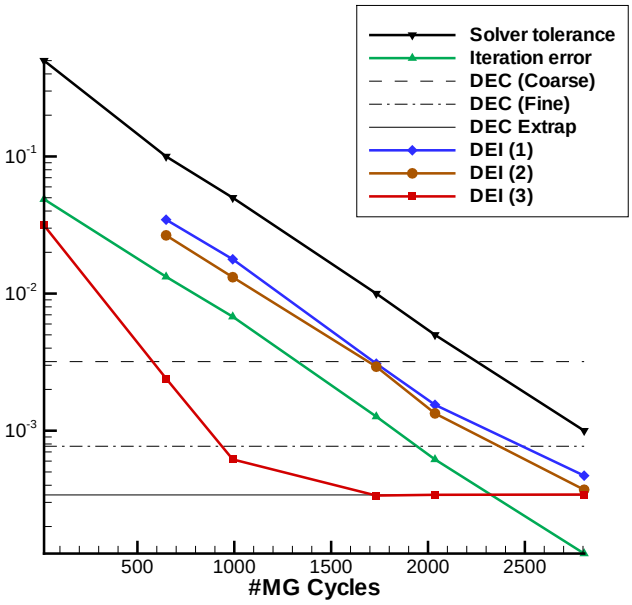

(b)

Figure 8: 2D Euler equations, quad-based uniform grid. (a): Analysis of dynamic truncation error accuracy and (b) dynamic τ-extrapolation.

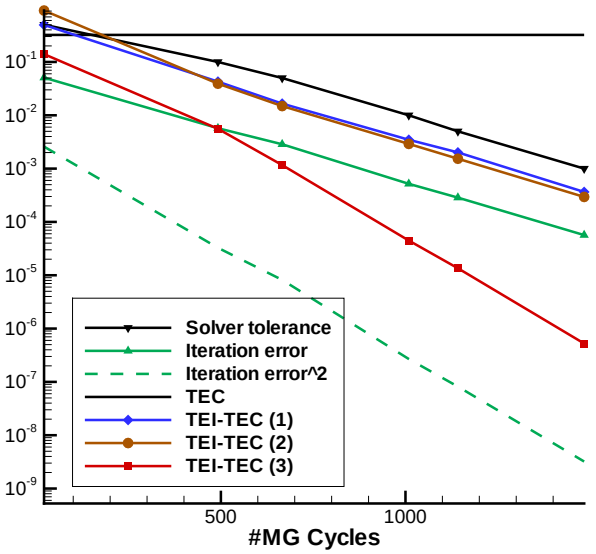

(a)

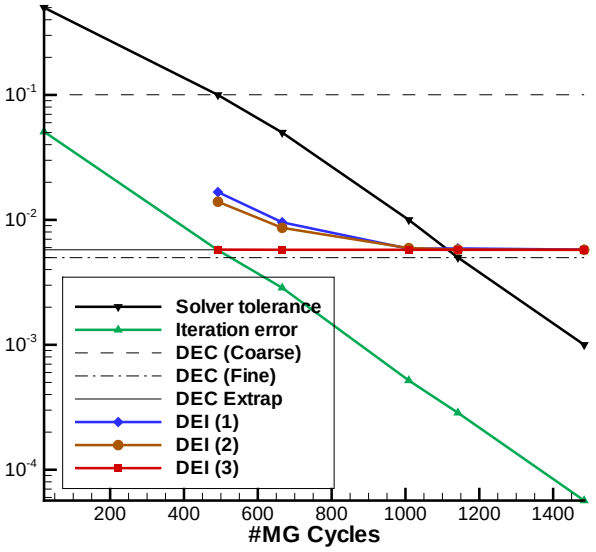

(b)

Figure 9: 2D Euler equations, quad-based distorted grid. (a): Analysis of dynamic truncation error accuracy and (b) dynamic τ-extrapolation.

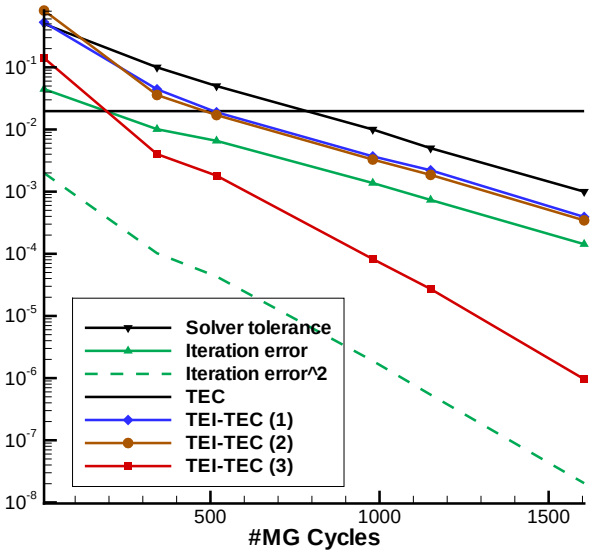

(a)

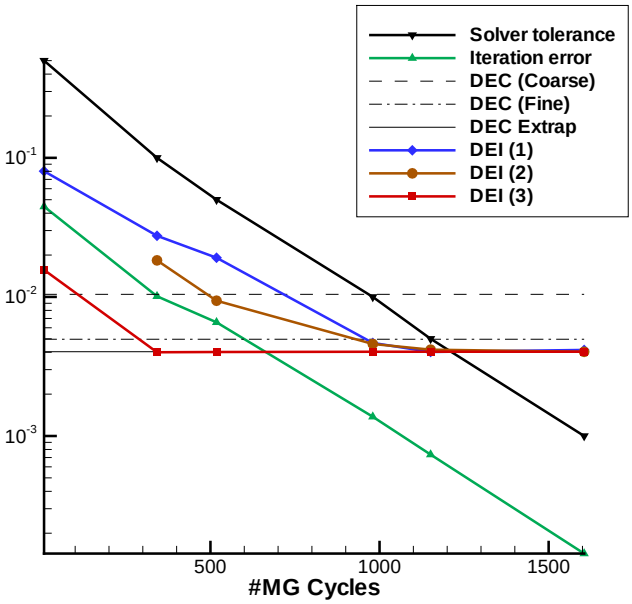

(b)

Figure 10: 2D Euler equations, triangle-based uniform grid. (a): Analysis of dynamic truncation error accuracy and (b) dynamic τ-extrapolation.

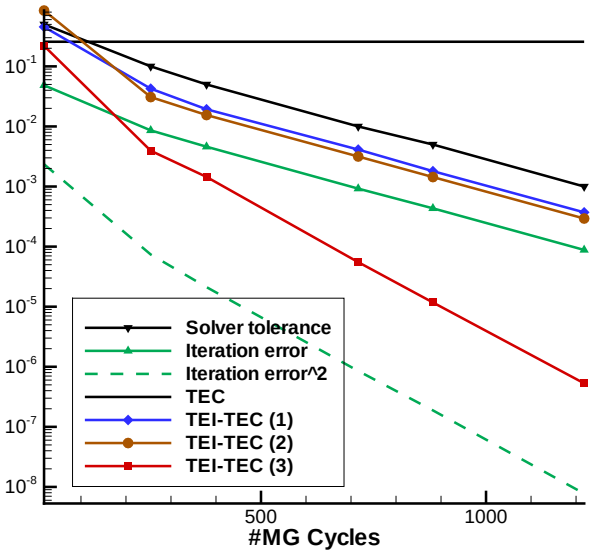

(a)

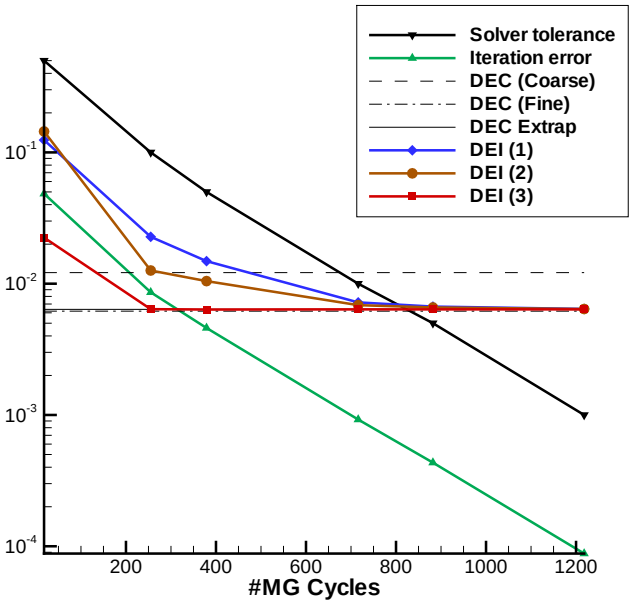

(b)

Figure 11: 2D Euler equations, triangle-based distorted grid. (a): Analysis of dynamic truncation error accuracy and (b) dynamic τ-extrapolation.

5. Conclusions

Dynamic τ-estimation has been successfully performed on finite difference solvers as well as in a finite volume solver on uniform and distorted grids. Conditions on the order of accuracy of the restriction operators and the magnitude of the iteration error to ensure accurate estimations have been derived and verified numerically on the scalar Poisson equation and on Euler equations. In this approach, a special attention has been paid to the use of non-converged solutions to estimate the truncation error in the early stages of the iterative procedure. The results demonstrated that if the restriction operators are chosen carefully, then the accuracy of the estimation increases quadratically with the decreasing of the iteration error. Otherwise, the estimation is accurate as long as the magnitude of the iteration error remains lower than the truncation error. In this paper, a direct application is presented, dynamic τ-extrapolation, and we demonstrated that it can be performed from a non-converged τ-estimation. The latter conclusion is of importance as for a given accuracy, important savings in terms of computational time may be obtained.

Appendix A. Accuary of τ-estimation and τ-extrapolation approaches

We analysed the magnitude of the error in the estimation as the mesh spacing is reduced for the 1D and 2D scalar problems when the solution is converged. In this aim, a set of successively refined grids was built from $imax = 9$ to $imax = 65$, by performing edge bisection both for uniform and distorted grids, thus following the requirements of Oberkampf [29] for a *systematic grid refinement* study.

The L_2 norm of the discretisation error, the exact truncation error and the error in the estimation $\|\frac{1}{1-\rho^p}\tau_h^H - \tau^H\|_{L_2}$ have been computed and are reported in Fig. A.12-A.13 for uniform and distorted grids and for both 1D and 2D Burgers' equations.

When the second order discretisation is used in conjunction with injection to restrict the solution, Eq.6 holds with $p = q = 2$ on uniform grids. Then, the error in the estimation is of the order of $\min(s, p + q)$. When injection is used to transfer the solution from fine to coarse mesh, $s = \infty$ and the estimation is accurate. However, when the second-order $s = 2$ operator is used, the estimation of the local truncation error is no longer accurate because the exact truncation error for this specific problem is also of the order of two.

In the case of distorted grids, the discretisation error maintains a second order accuracy while the truncation error drops to first order accuracy, which is a known issue of the discretisation on bad quality meshes (see Katz [32]). In this case, as can be seen in Fig.A.12(b) and Fig.A.13(b) for 1D and 2D scalar problems respectively, when an accurate restriction operator is used (e.g. injection), the error in the estimation drops to second order which is one order of magnitude higher than the exact truncation error itself.

τ-extrapolation results are shown in Fig.A.14 and Fig.A.15 for the 1D and 2D scalar equations and for uniform and distorted grids. The discretisation error is computed both for the initial problem and the extrapolated problem where the truncation error estimate is added as a source term to the original equations. The tendency follows the previous analysis: when a second order restriction operator is used to compute the truncation error estimate, then no particular gain can be obtained, whereas if injection is used, the extrapolated problems reaches a fourth order accuracy.

The extension to system of equations is straightforward, and truncation error maps for all conservative equations of the MMS problem are displayed in Fig.A.16, using a 9×9 triangle-

based distorted grid. It can be seen that, even for this very bad quality grid, the shape of the truncation error is well predicted.

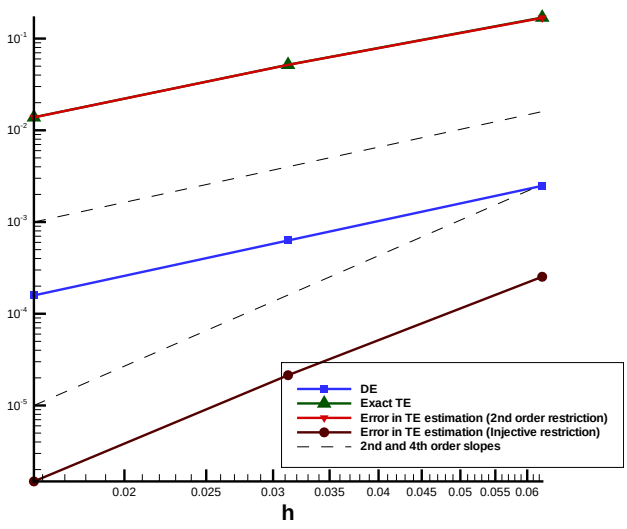

(a)

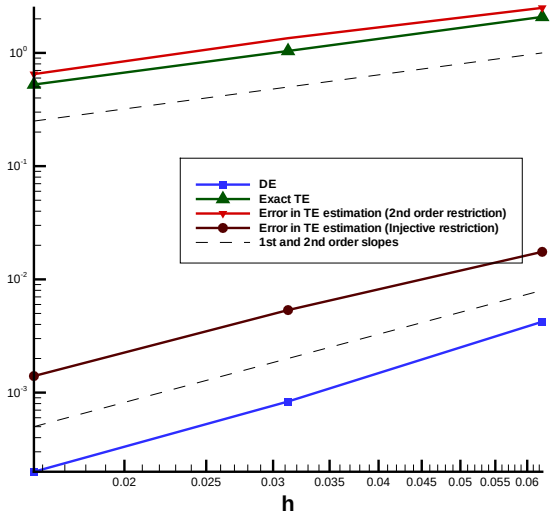

(b)

Figure A.12: $\|.\|_{L_2}$ of the DE, TE and error in the TE estimate for 1D (a): uniform, (b): distorted grids.

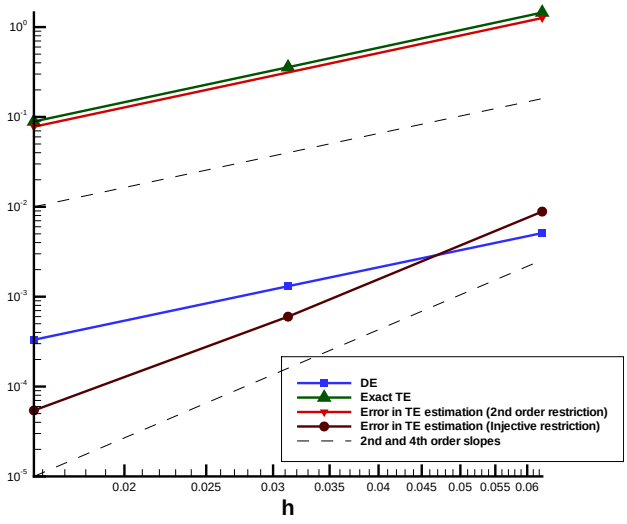

(a)

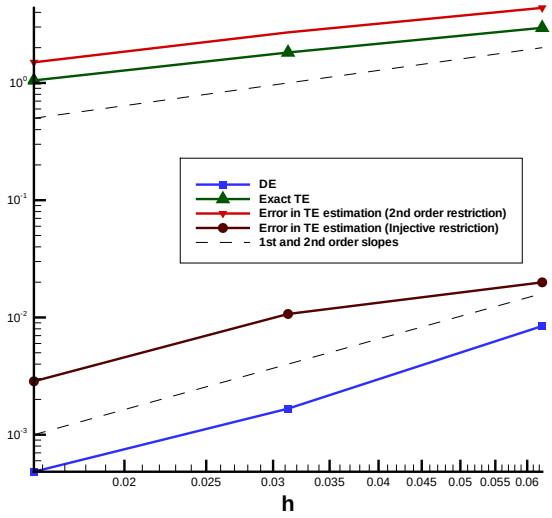

(b)

Figure A.13: $\|.\|_{L_2}$ of the DE, TE and error in the TE estimate for 2D (a): uniform, (b): distorted grids.

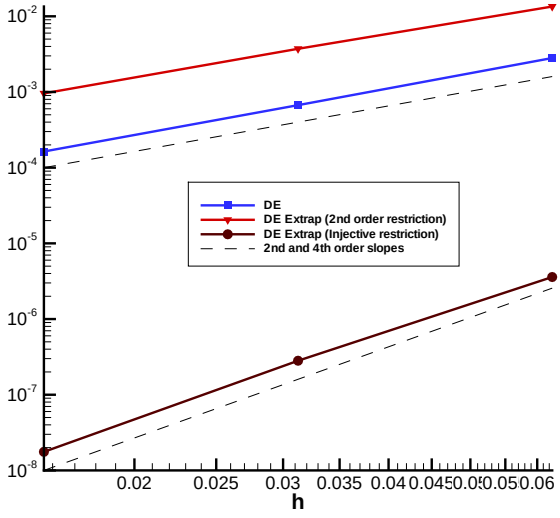

(a)

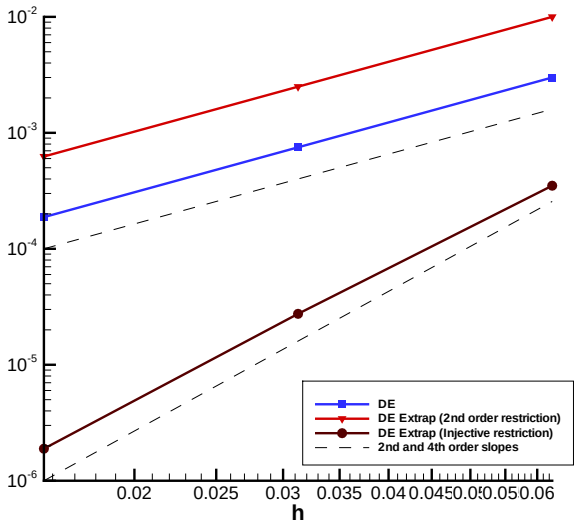

(b)

Figure A.14: $\|.\|_{L_2}$ of the DE and extrapolated DE for 1D (a): uniform, (b): distorted grids.

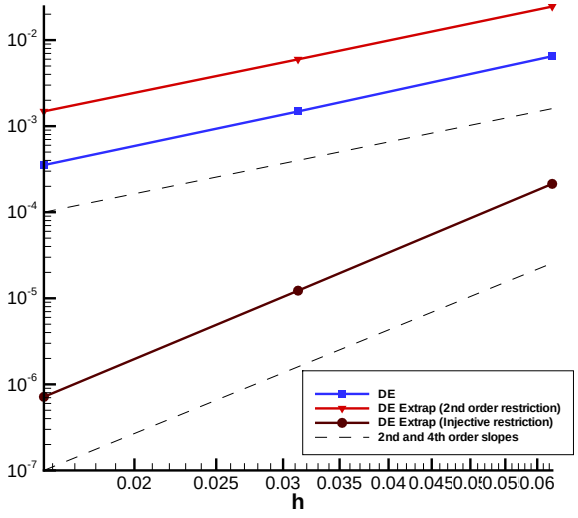

(a)

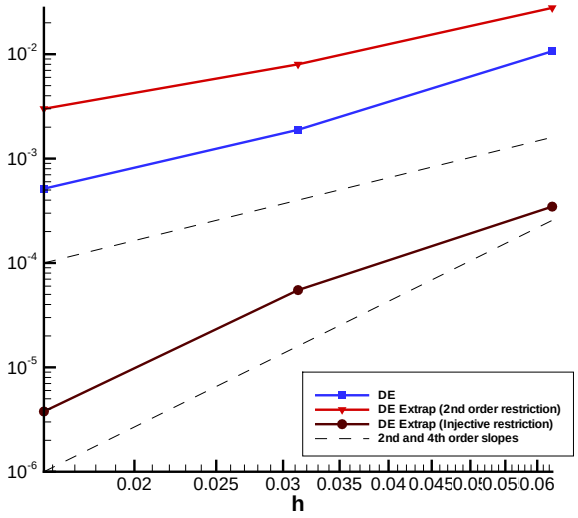

(b)

Figure A.15: $\|.\|_{L_2}$ of the DE and extrapolated DE for 2D (a): uniform, (b): distorted grids.

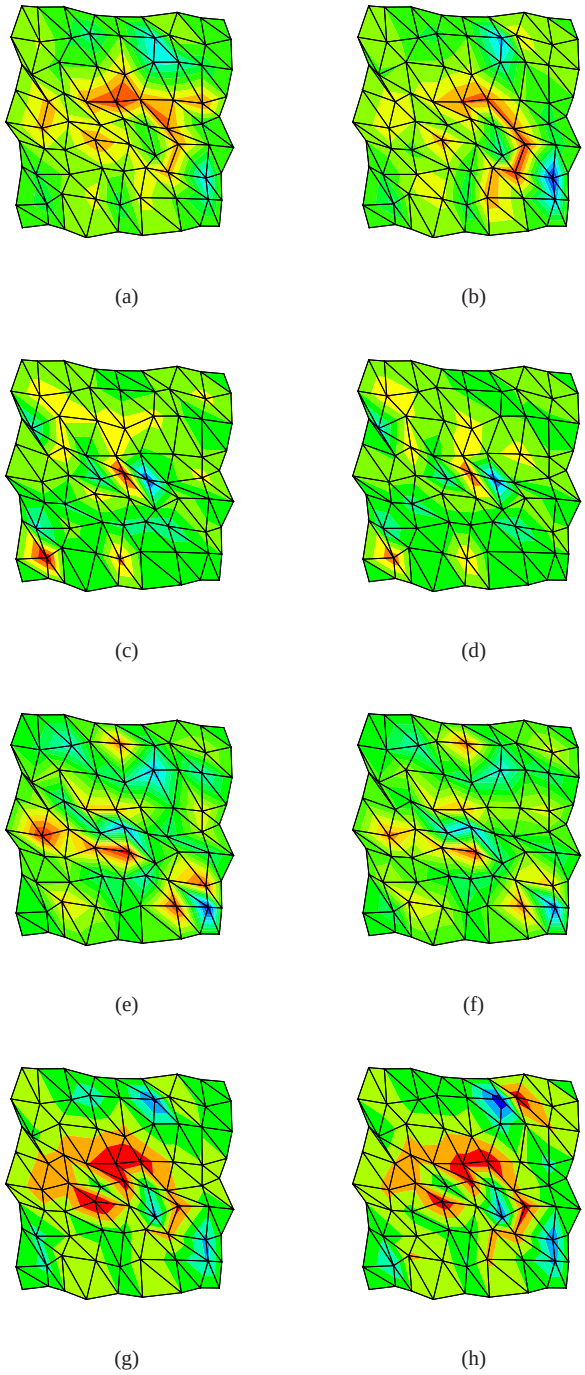

Figure A.16: Truncation error contours for the Euler MMS problem. Left column: exact, and right column: estimation of the truncation error. Rows: continuity, x- and y-momentum and energy equation respectively.

References

[1] C. J. Roy, *Review of discretisation error estimators in scientific computing*, AIAA Paper 2010-126, 2010

[2] L. F. Richardson, *The Approximate Arithmetical Solution by Finite Differences of Physical Problems Involving Differential Equations, with an Application to the Stresses in a Masonry Dam*, Transactions of the Royal Society of London, Series A, Vol. 210, pp. 307-357, 1910.

[3] W. Briggs, V. E. Henson, S. McCormick, *A Multigrid Tutorial*, second edition, Society for Industrial and Applied Mathematics, Philadelphia, PA, 2000

[4] U. Trottenberg, C. Oosterlee, A. Schüler, *Multigrid*, first edition, Academic Press, 2000

[5] A. Brandt, *Multigrid Techniques: 1984 Guide with applications to fluid dynamics*, revised edition, Society for Industrial and Applied Mathematics, 2011

[6] C. Ilinca, X. D. Zhang, J.-Y. Trépanier, R. Camarero, *A comparison of three error estimation techniques for finite-volume solutions of compressible flows*, Computer Methods in Applied Mechanics and Engineering, 189 (4), pp. 1277-1294, 2000

[7] M. Garbey, W. Shyy, *42. Error Estimation, Multilevel Method and Robust Extrapolation in the Numerical Solution of PDEs*, Fourteenth International Conference on Domain Decomposition Methods

[8] T. S. Phillips, C. J. Roy, *Evaluation of Extrapolation-Based discretisation Error and Uncertainty Estimators*, AIAA Paper 2011-215, 2011

[9] T. I.-P. Shih, B. R. Williams, *Development and evaluation of an a posteriori method for estimating and correcting grid-induced errors in solutions of the Navier-Stokes equations*, AIAA Paper 2009-1499, 2009

[10] M. B. Giles, N. A. Pierce, *Adjoint equations in CFD: duality, boundary conditions and solution behaviour*, AIAA Paper 97-1850, 1997

[11] D. A. Venditti, D. L. Darmofal, *Adjoint Error Estimation and Grid Adaptation for Functional Outputs: Application to Quasi-One- Dimensional Flow*, Journal of Computational Physics, 164 (1), pp. 204-227, 2000

[12] J. D. Hoffman, *Relationship between the Truncation Errors of Centered Finite-Difference Approximations on Uniform and Nonuniform Meshes*, Journal of Computational Physics, 46 (3), pp. 469-474, 1982

[13] B. P. Leonard, *Comparison of Truncation Error of Finite-Difference and Finite-Volume Formulations of Convection Terms*, NASA Technical Memorandum 105861, ICOMP-92-19, 1992

[14] Y. N. Jeng, J. L. Chen, *Truncation error analysis of the finite volume method for a model steady convective equation*, Journal of Computational Physics, 100 (1), pp. 64-76, 1992

[15] S. F. Hagen, *Estimation of the Truncation Error for the Linearized, Shallow Water Momentum Equations*, Engineering with Computers, 17, pp. 354-362, 2001

[16] Y. Kallinderis, C. Kontzialis, *A priori mesh quality estimation via direct relation between truncation error and mesh distortion*, Journal of Computational Physics, 228 (3), pp. 881-902, 2009

[17] M. J. Berger, *Adaptive Finite Difference Methods in Fluid Dynamics*, Mathematics and Computers, Courant Institute of Mathematical Sciences, New York University, New York, 1987

[18] K. Bernert, *τ-Extrapolation-Theoretical foundation, numerical experiment, and application to Navier-Stokes equations* SIAM Journal on Scentific Computing, 18 (2), pp. 460-478, 1997

[19] S. R. Fulton, *On the accuracy of multigrid truncation error estimates*, Electronic transactions on numerical analysis, 15, pp. 29-37, 2003

[20] F. Fraysse, J. De Vicente, E. Valero, *The estimation of truncation error by τ-estimation revisited*, Journal of Computational Physics, Vol. 231 (9), pp. 3457-3482, 2012

[21] A. Syrakos, A. Goulas, *Estimate of the truncation error of finite volume discretisation of the Navier-Stokes equations on colocated grids*, International Journal for Numerical Methods in Fluids, 50 (1), pp. 103-130, 2006

[22] A. Syrakos, G. Efthimiou, J. G. Bartzis, A. Goulas, *Numerical experiments on the efficiency of local grid refinement based on truncation error estimates*, Journal of Computational Physics, Vol. 231 (20), pp. 67256753, 2012

[23] F. Fraysse, E. Valero, J. Ponsín, *Comparison of Mesh Adaptation Using the Adjoint Methodology and Truncation Error Estimates*, AIAA Journal, 50 (9), pp. 1920-1932, 2012

[24] T. Gerhold, V. Hannemann, D. Schwamborn, *On the Validation of the DLR-TAU Code*, New Results in Numerical and Experimental Fluid Mechanics, Notes on Numerical Fluid Mechanics, 72, pp. 426-433, 1999

[25] A. Jameson, W. Schmidt, E. Turkel, *Numerical Solution ofthe Euler Equations by Finite Volume Methods Using Runge-Kutta Time-Stepping Schemes*, AIAA Paper 81-1259, 1981

[26] T. S. Phillips and C. J. Roy, *Residual Methods for Discretization Error Estimation*, AIAA Paper 2011-3870, 2011

[27] P. Wesseling, *An introduction to multigrid methods*, John Wiley & Sons, 1991

[28] P. J. Roache, *Verification and validation in computational science and engineering*, Albuquerque, NM: Hermosa Publishers, 1998

[29] W. L. Oberkampf, C. J. Roy, *Verification and Validation in Scientific Computing*, Cambridge University Press, Cambridge, 2010

[30] C. J. Roy, *Review of code and solution verification procedures for computational simulation*, Journal of Computational Physics, 205 (1), pp. 131-156, 2005
[31] S. Balay, J. Brown, K. Buschelman, V. Eijkhout, W. D. Gropp, D. Kaushik, M. G. Knepley, L. Curfman McInnes, B. F. Smith, H. Zhang, *PETSc Users Manual*, ANL-95/11 - Revision 3.3, Argonne National Laboratory, 2012
[32] A. Katz, V. Sankaran, *Mesh quality effects on the accuracy of CFD solutions on unstructured meshes*, Journal of Computational Physics, 230 (20), pp. 7670-7686, 2011